Supporting information

The Effect of Chlorination and Position Isomerization of Benzotriazole-based Acceptors on High-Voltage Organic Solar Cells based on Dithienobenzodithiophene (DTBDT)-Containing Polymer Donor

Jinge Zhu[1,2,#], Mengzhen Du[1,2,#],Ailing Tang[2], Yuhan Meng[1,2], Chao Li*[3], Qing Guo*[4], Erjun Zhou*[1,2]*

[1] College of Materials Science and Engineering, Zhengzhou University, Zhengzhou 450001, China.
[2] National Center for Nanoscience and Technology, Beijing 100190, China.
[3] Zhongyuan Critical Metals Laboratory, Zhengzhou University, Zhengzhou 450001, China.
[4] Henan Institute of Advanced Technology, Zhengzhou University, Zhengzhou 450003, China.
E-mail: tangal@nanoctr.cn; zhouej@nanoctr.cn
[#] Contributed equally to this work

Materials and Synthesis

All the reagents were purchased from commercial sources and used without further purification. PE56,[1] BTA5,[2] BTA5-Cl and Cl-BTA5[3] were synthesized according to previous works.

Experimental section

Fabrication of organic photovoltaic device

Organic solar cells (OSCs) were fabricated with a conventional structure of ITO/PEDOT: PSS/active layers/PFN-Br/Ag. Clean the glass substrates coated with ITO using detergent deionized water and ethanol for 25 minutes each under the room temperature. A 30 nm thick PEDOT: PSS layer was firstly spin-casted on top of the ITO substrates at a speed of 3000 rpm for 35 s and then annealed at 150 ℃ in an air atmosphere for 10 min. The Donor: Acceptor (D: A) ratio of 1: 1 (w/w) for PE56: BTA5 was dissolved in CF (chloroform) with a donor concentration of 7 mg/mL. The D: A ratio of 1.2: 1 (w/w) for PE56: BTA5-Cl was dissolved in CF with a donor concentration of 6 mg/mL. The D: A ratio of 1: 1 (w/w) for PE56: Cl-BTA5 was dissolved in CF with a donor concentration of 7 mg/mL, and 0.5% (v/v) DPE (diphenyl ether) was added as a solvent additive. Three active layers were spin-coated on the top of PEDOT: PSS at speeds of 2000 rpm, 3000 rpm and 2000 rpm, respectively, and then annealed at 170 ℃ for 10 minutes. The thicknesses of the three blend films are 95 nm, 90 nm, and 93 nm, respectively. This process was carried out in a glove box filled with N2. A PFN-Br layer was spin-coated on the top of all the active layers at 3000 rpm for 35 s in an N2-filled glove box, which was dissolved in methanol at a concentration of 0.5 mg/mL. Finally, under vacuum conditions of 3×10^{-4} Pa, silver with a thickness of 100 nm was thermally deposited as a metal electrode.

Measurements and characterizations

Molecular weights of the polymers were measured on Agilent Technologies PL GPC 220 high-temperature-chromatograph at 150 ℃ using a calibration curve of polystyrene standards. UV-vis spectra were tested by UV-3600i PLUS (Shimadzu Corporation). The film specimens were spin-coated on quartz substrate. The concentration of solution specimens was 0.01 mol mL^{-1}.

The *J–V* curves were measured using a Zolix Solar IV-150A-ZZU system. Light intensity was calibrated with a Zolix QE-B1 Si-based solar cell and the photocurrent was measured under AM 1.5 G illumination at 100 $mW \cdot cm^{-2}$ using a Zolix HPS-300XA solar simulator. All the devices were not encapsulated and they were tested in glovebox filled with N_2. The EQE spectrum were measured by a Zolix SCS10-X150-DSSC-ZZU system. The film specimens were spin-coated on quartz substrate and then the photoluminescence (PL) measurement was performed using a Hitachi F-7000 spectrofluorophotometer. The film specimens were spin-coated on quartz substrate.

The height images of blend films were carried out using the Dimension 3100 atomic force microscopy (AFM) on samples in actual device configuration. The scans were carried out on 4×4 μm^2 surface areas, using tapping mode. Two-dimensional grazing incidence wide-angle X-ray scattering (2D-GIWAXS) analyses were investigated at the XEUSS SAXS/WAXS equipment. Illuminate the film at a fixed incidence angle, where the wavelength of the X-ray is 1.542 Å. All active layers were spin-coated on silicon substrate. The contact angle was tested by JY-82C (Chengde Dingsheng).

Hole-only and electron-only devices were fabricated by using the device structures of glass/ITO/PEDOT:PSS/active layer/Au and glass ITO/ZnO/active layer/PFN-Br/Ag, respectively. The hole and electron mobilities were approximated by the Mott-Gurney equation:

$$J = \frac{9}{8}\varepsilon_0\varepsilon_r\mu\frac{V^2}{L^3}$$

where J stands for current density, ε_0 is the permittivity of free space (8.85×10^{-12} $C \cdot V^{-1} \cdot m^{-1}$), ε_r is the relative dielectric constant of the transport medium (assuming that

of 3.0), μ is the charge mobility, V is the internal potential in the device, and L is the thickness of the active layer. The thickness of the active layer was measured on the FILMETRICS F20-EXR optical profilometer. The average carrier mobility values have been listed in SI to rule out device-to-device differences. The average electron mobility and the hole mobility calculated from five cells for PE56: BTA5, PE56: BTA5-Cl, and PE56: Cl-BTA5 are $(2.02\pm0.45)\times10^{-4}$ / $(2.99\pm0.57)\times10^{-4}$, $(3.23\pm0.66)\times10^{-4}$/$(4.02\pm0.61)\times10^{-4}$, and $(3.87\pm0.55)\times10^{-4}$ /$(4.82\pm0.43)\times10^{-4}$ cm^2 V^{-1} s^{-1}, respectively.

Supporting figures and tables

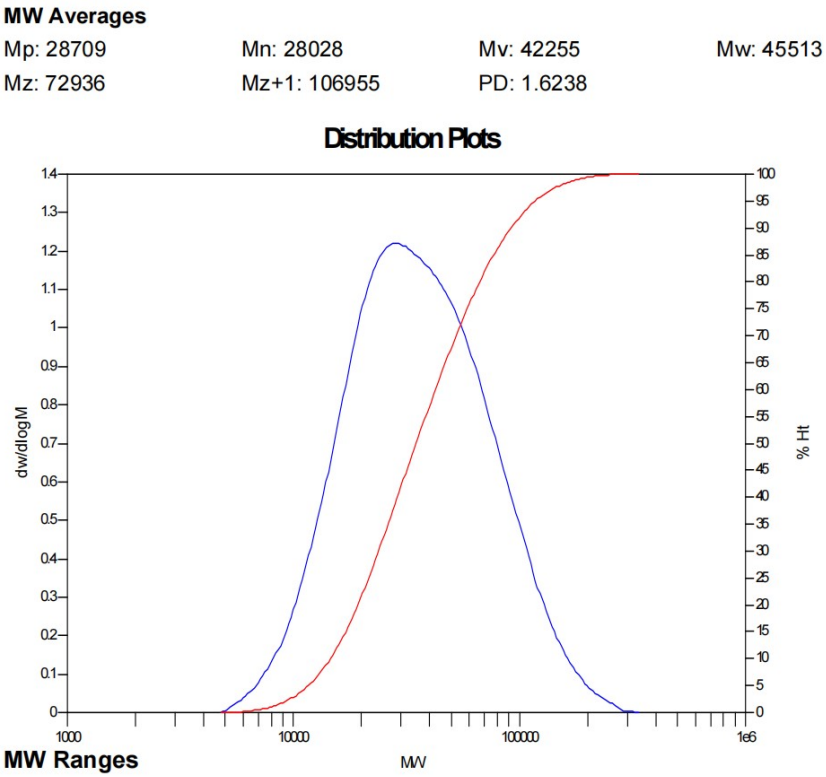

Figure S1. GPC trace of PE56.

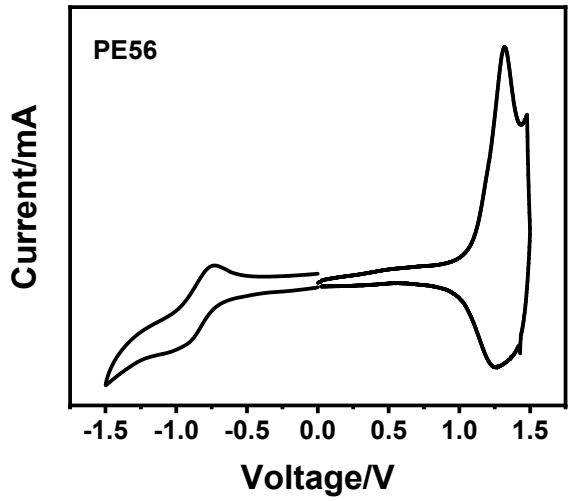

Figure S2. CV curve of PE56.

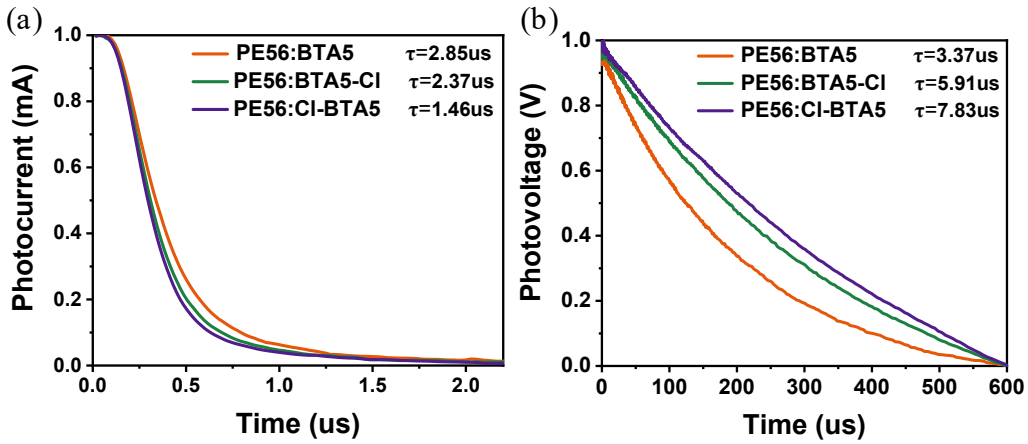

Figure S3. Normalized TPV of the three devices (a); Normalized TPC of the three devices (b).

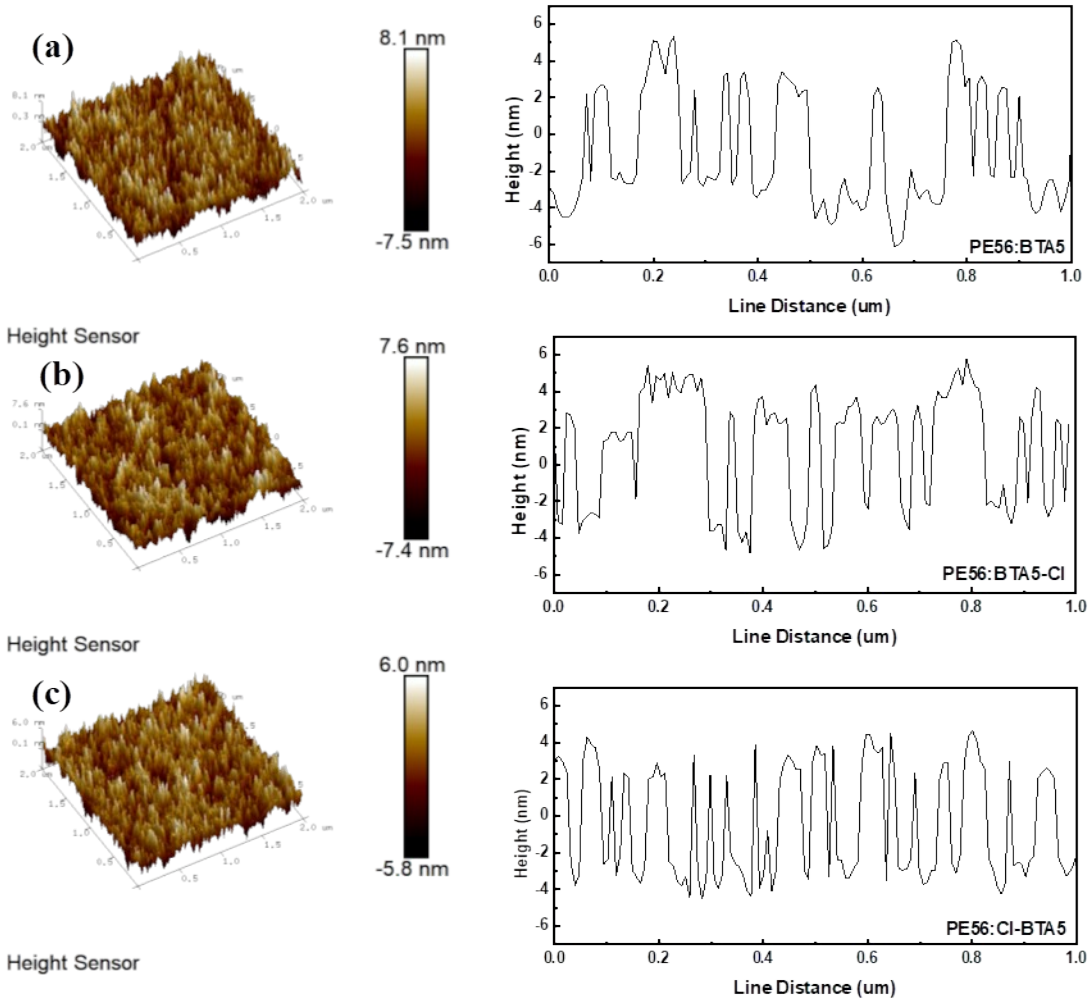

Figure S4. 3D AFM height images and height distribution plots of three devices.

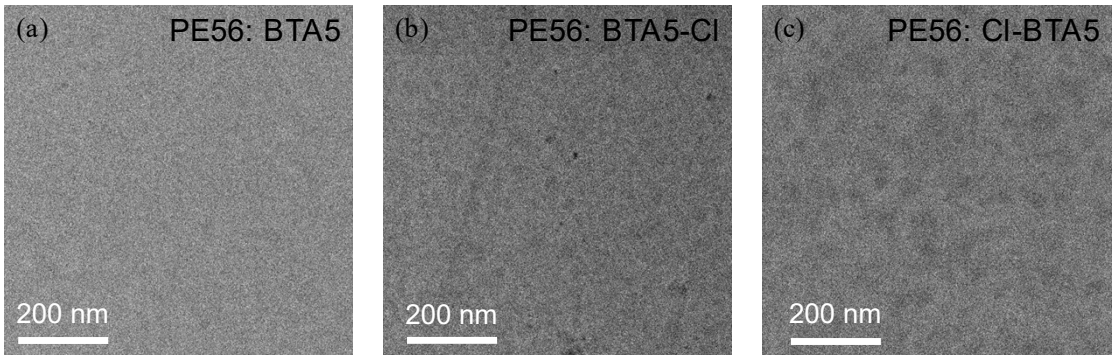

Figure S5. TEM images of PE56:BTA5 (a), PE56: BTA5-Cl (b) and PE56: Cl-BTA5 (c) blend films.

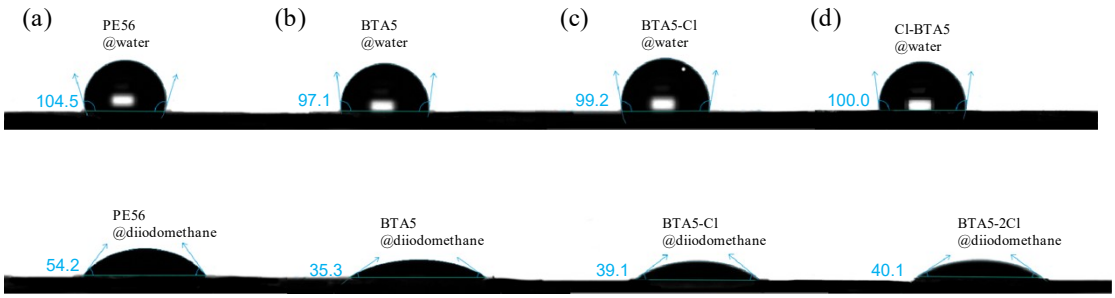

Figure S6. The contact angles of water and diiodomethane on the surface of PE56 (a), BTA5 (b), BTA5-Cl (c) and Cl-BTA5 (d).

Table S1. Photophysical properties and energy levels of PE56, BTA5, BTA5-Cl, and Cl-BTA5.

	λmax, solution(nm)	λmax, film (nm)	*Eg* (eV)	HOMO (eV)	LUMO (eV)
PE56	588	591	1.98	-5.45	-3.47
BTA5	618	643	1.84	-5.55	-3.71
BTA5-Cl	623	647	1.77	-5.65	-3.88
Cl-BTA5	618	650	1.78	-5.75	-3.97

Table S2. Device optimization based on PE56: BTA5.

	D: A	V_{OC} (V)	J_{SC} (mA cm^{-2})	FF (%)	PCE (%)
D=7mg/ml	1:1	1.250	7.31	59.45	5.44
170°C10min	1:1.5	1.244	7.17	57.92	5.16
3000rpm	1.5:1	1.239	7.08	56.73	4.98
	1:1.2	1.232	7.39	57.56	5.24

	additive	Annealing (°C)	V_{OC} (V)	J_{SC} (mA cm^{-2})	FF (%)	PCE (%)
D:	/	150	1.256	7.15	57.93	5.20
7mg/ml	/	170	1.250	7.31	59.45	5.44
D: A	/	190	1.246	7.28	58.03	5.26
1:1	0.5%DPE		1.233	6.82	57.76	4.86
3000	0.5%CN	170	1.242	7.11	56.93	5.03
rpm	0.5%DIO		1.257	6.63	57.69	4.81

	Concentration (D=mg/ml)	V_{OC} (V)	J_{SC} (mA cm-2)	FF (%)	PCE (%)

D:A=1:1	6	1.247	7.13	58.82	5.23
170℃10min	7	1.250	7.31	59.45	5.44
3000rpm	8	1.252	7.09	59.16	5.25

Table S3. Device optimization based on PE56: BTA5-Cl.

	D: A	V_{OC} (V)	J_{SC} (mA cm^{-2})	FF (%)	PCE (%)
D=7mg/ml	1:1	1.197	11.44	65.65	8.99
170℃10min	1:1.5	1.192	11.16	66.01	8.78
	1.5:1	1.195	11.32	67.19	9.09
2000rpm	1.2:1	1.198	11.49	67.62	9.31

	additive	Annealing (℃)	V_{OC} (V)	J_{SC} (mA cm^{-2})	FF (%)	PCE (%)
D	/	150	1.193	11.19	66.43	8.87
7mg/ml	/	170	1.200	11.91	68.00	9.71
D: A	/	190	1.195	11.55	66.79	9.22
1.2:1	0.5%DPE		1.204	11.79	68.11	9.67
2000	0.5%CN	170	1.191	11.26	66.19	8.88
rpm	0.5%DIO		1.187	11.14	66.23	8.76

	Concentration (D=mg/ml)	V_{OC} (V)	J_{SC} (mA cm-2)	FF (%)	PCE (%)
D:A=1.2:1	6	1.200	11.91	68.00	9.71
170℃10min	7	1.198	11.75	67.19	9.46
2000rpm	8	1.192	11.74	67.84	9.50

Table 4. Device optimization based on PE56: Cl-BTA5.

	D: A	V_{OC} (V)	J_{SC} (mA cm^{-2})	FF (%)	PCE (%)
D=7mg/ml	1:1	1.182	13.21	67.79	10.58
170℃10min	1:1.5	1.174	13.20	64.88	10.05
	1.5:1	1.176	12.89	67.24	10.19
3000rpm	1.2:1	1.178	13.13	67.17	10.38

	additive	Annealing (℃)	V_{OC} (V)	J_{SC} (mA cm^{-2})	FF (%)	PCE (%)
D	/	150	1.178	12.94	68.15	10.38

7mg/ml	/	170	1.182	13.21	67.79	10.58
D: A	/	190	1.179	12.73	67.84	10.18
1:1	0.5%DPE		1.170	13.52	70.67	11.18
3000	0.5%CN		1.169	12.76	68.83	10.26
rpm	0.5%DIO	170	1.171	12.47	70.57	10.30
	0.25%DPE		1.174	13.27	69.75	10.86
	0.5%DPE		1.170	13.52	70.67	11.18
	1%DPE		1.166	13.57	68.27	10.80

	Concentration (D=mg/ml)	V_{OC} (V)	J_{SC} (mA cm^{-2})	FF (%)	PCE (%)
D: A=1:1	6	1.168	13.57	69.90	11.07
0.5%DPE170℃	7	1.170	13.52	70.67	11.18
3000rpm	8	1.171	13.39	69.76	10.94

Table S5. The contact angles (θ) and surface tension (γ) of pure film and interaction parameters (χ) between polymer and donors.

Film	θwater (deg)	θdiiodomethane (deg)	γ(mN m-1)	χ
PE56	104.5	54.2	33.28	
BTA5	97.1	35.3	43.29	0.66
BTA5-Cl	99.2	39.1	41.69	0.47
BTA5-2Cl	100.0	40.1	41.38	0.44

Table S6. Detailed GIWAXS data of PE56: BTA5/BTA5-Cl/Cl-BTA5 blend films.

Blends	OOP				IP			
	(010)				(100)			
	q (Å^{-1})	d-spacing (Å)	FWHM (Å^{-1})	CCL (Å)	q (Å^{-1})	d-spacing (Å)	FWHM (Å^{-1})	CCL (Å)
PE56:BTA5	1.783	3.52	0.21	28.49	0.31	20.46	0.087	67.13
PE56:BTA5-Cl	1.779	3.53	0.22	26.07	0.31	20.59	0.088	66.07
PE56:Cl-BTA5	1.772	3.54	0.18	33.18	0.30	21.29	0.083	70.37

Table S7. Detalied parameters of reported OSCs based on DTBDT-polymer donor.

Active layer	V_{OC} (V)	J_{SC} (mA cm^{-2})	FF (%)	PCE (%)	Reference
PE55:BTA3	1.28	10.59	64.20	9.19	[4]

PDBQx-TCl: BTA3-4F: PY-IT	0.934	24.9	79.8	18.6	[5]
PDTBDT: PYF-T-O	0.84	24.77	64.52	13.38	[6]
P-PhS: BTP-eC9	0.88	25.4	75.6	11.4	[7]
M-PhS: BTP-eC9	0.84	25.4	75.6	15.9	
PE55:Y6	0.82	24.34	69.48	13.78	[1]
PE56:Y6	0.86	24.06	69.78	14.49	
PE51	0.79	24.11	69.75	13.34	[8]
PE52	0.80	25.36	71.94	14.61	
PE53	0.83	23.64	69.84	13.72	
PDBT-F:IT-4F	0.81	20.9	59	10	[9]
PDBT-Cl:IT-4F	0.82	22.3	69	12.6	
PDBT-2F:IT-4F	0.87	20.6	57	10.2	
PDBT-2Cl:IT-4F	0.99	15.1	42	6.2	
PE64: ITIC	0.79	12.43	48	4.69	[10]
PE65: ITIC	0.94	13.91	67	8.88	
DTBDT-S-C8-TTR: PC71BM	0.88	16.24	61	8.71	[11]
PDTBDT-SFBT: PC71BM	0.78	14.63	67.68	7.71	[12]
DTBDT-TzVTz: PC71BM	0.79	13.17	64	6.73	[13]
PDTBDT-D-DPP: PC71BM	0.68	12.70	67.10	5.79	[14]
PDTBDT-T: Y6	0.78	24.21	65.81	12.71	[15]
PDTBDT-T-TCl: Y6	0.86	24.46	71.65	15.63	
PDBT-F:IT-M	0.97	17.02	63.71	10.52	[16]
PDBT-F: IDIC	0.87	17.65	71.50	11.02	
PDTBDT-T-DTNT: PC71BM	0.6	10.15	65.16	3.97	[17]
PDTBDT-TE-DTNT:	0.7	16.09	67.19	7.57	

PC71BM					
PDBT-T1:SdiPBI-Se:TIC-TH	0.94	15.40	71.3	10.3	[18]
PDTBDT-SSBTEH: ITIC	0.82	13.76	63.50	7.16	[19]
PDTBDT-SFBTEH: ITIC	0.94	13.81	66.30	8.61	
PDBT-T1:IC-C6IDT-IC	0.89	15.05	63	8.71	[20]
PDBT-T1: IC-1IDT-IC	0.92	13.39	60	7.39	[21]
PDBT-T1:2C-1IDT-IC	1.02	5.28	48.0	2.58	
PDBT-T1: IC-C61DT-IC	0.85	15.85	68	9.20	
PDBT-T1: IDIC	0.834	16.98	73.2	10.37	[22]
PDBT-T1: SdiPBI-BT	0.95	10.32	67.6	6.71	[23]
PDBT-T1: diPBI-BT	0.99	9.67	59.8	5.84	
PDBT-DTT: ITCPTC	0.79	15.6	68.2	8.74	[24]
PDTBDT-TPTI: ITIC	0.86	13.34	60.0	6.91	[25]
PDBT(E)BTz-p: IT-4F	0.98	14.38	48.2	6.96	[26]
PDBT(E)BTz-d: IT-4F	0.95	14.68	54.5	7.81	
PDBT(E)BTz-p: PBDB-T: IT-4F	0.86	19.90	72.5	12.5	
PDBT(E)BTz-d: PBDB-T: IT-4F	0.86	20.59	74.9	13.4	
PDTBDT-BZ: BDTD-Ph	0.884	13.29	55.4	6.50	[27]
PDTBDT-BZ: BDTD-Na	0.864	12.86	44.5	4.95	
PDTBDT-BZ: TBDB-Ph	0.913	13.41	51.8	6.20	
PDTBDT-BZ: TBDT-Na	0.879	11.24	54.4	5.38	

References

(1) Zhou, J.; Guo, Q.; Zhang, B.; Cheng, S.-X.; Hao, X.-T.; Zhong, Y.; Tang, A.; Sun, X.; Zhou, E. Improving the Photovoltaic Performance of Dithienobenzodithiophene-Based Polymers Via Addition of an Additional Eluent in the Soxhlet Extraction Process. *ACS Appl. Mater. Interfaces* **2022**, *14* (46), 52244-52252.

(2) Wang, X.; Tang, A.; Yang, J.; Du, M.; Li, J.; Li, G.; Guo, Q.; Zhou, E. Tuning the Intermolecular Interaction of A2-A1-D-A1-A2 Type Non-Fullerene Acceptors by Substituent Engineering for Organic Solar Cells with Ultrahigh Voc of ~1.2 V. *Sci. China Chem.* **2020**, *63* (11), 1666-1674.
(3) Zuo, K.; Dai, T.; Guo, Q.; Wang, Z.; Du, M.; Wang, H.; Tang, A.; Zhou, E.; Guo, Q.; Zhang, Y. Ptq10-Based Organic Photovoltaics with a High V Oc of~ 1.2 V Via Chlorination of Benzotriazole-Based Nonfullerene Acceptors. *ACS Appl. Energy Mater.* **2022**, *5* (11), 14271-14279.
(4) Li, X.; Wang, Z.; Tang, A.; Guo, Q.; Liu, Y.; Du, M.; Zhou, E. Dithienobenzothiadiazole (Dtbt)-Based Polymers Enable Organic Solar Cells with Ultrahigh Voc of ≈1.3 v. *Macromol. Rapid Commun.* **2023**, *44* (12), 2300019.
(5) Xu, Y.; Wang, J.; Zhang, T.; Chen, Z.; Xian, K.; Li, Z.; Luo, Y.-H.; Ye, L.; Hao, X.; Yao, H.; et al. Suppression of Energy Disorder by Incorporating a Small-Molecule Acceptor into Binary All-Polymer Solar Cells. *Energy Environ. Sci.* **2023**, *16* (12), 5863-5870.
(6) Qiu, D.; Shi, Y.; Li, Y.; Zhang, J.; Lu, K.; Wei, Z. Conjugation Expansion Strategy Enables Highly Stable All-Polymer Solar Cells. *Chin. Chem. Lett.* **2023**, *34* (8), 108019.
(7) Zhang, L.; Zhu, X.; Deng, D.; Wang, Z.; Zhang, Z.; Li, Y.; Zhang, J.; Lv, K.; Liu, L.; Zhang, X.; et al. High Miscibility Compatible with Ordered Molecular Packing Enables an Excellent Efficiency of 16.2% in All-Small-Molecule Organic Solar Cells. *Adv. Mater.* **2022**, *34* (5), 2106316.
(8) Zhou, J.; Zhang, B.; Du, M.; Dai, T.; Tang, A.; Guo, Q.; Zhou, E. Side-Chain Engineering of Copolymers Based on Benzotriazole (Bta) and Dithieno[2,3-D;2′,3′-D′]Benzo[1,2-B;4,5-B′]Dithiophenes (Dtbdt) Enables a High Pce of 14.6%. *Nanotechnology* **2021**, *32* (22), 225403.
(9) Huang, J.; Xie, L.; Hong, L.; Wu, L.; Han, Y.; Yan, T.; Zhang, J.; Zhu, L.; Wei, Z.; Ge, Z. Significant Influence of Halogenation on the Energy Levels and Molecular Configurations of Polymers in Dtbdt-Based Polymer Solar Cells. *Mater. Chem. Front.* **2019**, *3* (6), 1244-1252.
(10) Zhou, J.; Zhang, B.; Zou, W.; Tang, A.; Geng, Y.; Zeng, Q.; Guo, Q.; Zhou, E. Chlorination of Dithienobenzodithiophene (Dtbdt) Based Polymers to Simultaneously Improve the Voc, Jsc and Ff of Non-Fullerene Organic Solar Cells. *Sustain. Energ. Fuels* **2020**, *4* (11), 5665-5673.
(11) Hong, J.; Choi, J. Y.; Kim, K.; Lee, N.-S.; Li, J.; Park, C. E.; An, T. K.; Kim, Y.-H.; Kwon, S.-K. Side Chain Engineering in Dtbdt-Based Small Molecules for Efficient Organic Photovoltaics. *Nanoscale* **2019**, *11* (29), 13845-13852.
(12) Zhang, X.; Wang, F.; Tong, J.; Zhang, M.; Guo, P.; Li, J.; Xia, Y.; Wang, C.; Wu, H. Systematically Investigating the Influence of Inserting Alkylthiophene Spacers on the Aggregation, Photo-Stability and Optoelectronic Properties of Copolymers from Dithieno[2,3-D:2′,3′-D′]Benzo[1,2-B:4,5-B′]Dithiophene and Benzothiadiazole Derivatives. *Polym. Chem.* **2019**, *10* (8), 972-982.

(13) Hong, J.; Wang, C.; Cha, H.; Kim, H. N.; Kim, Y.; Park, C. E.; An, T. K.; Kwon, S.-K.; Kim, Y.-H. Morphology Driven by Molecular Structure of Thiazole-Based Polymers for Use in Field-Effect Transistors and Solar Cells. *Chem. Eur. J.* **2019**, *25* (2), 649-656.
(14) Guo, P.; Miao, W.; Liu, G.; Tong, J.; Liang, Q.; Zhang, Y.; Li, M.; Li, J.; Wang, C.; Wang, E.; et al. Twisted Alkylthiothien-2-Yl Flanks and Extended Conjugation Length Synergistically Enhanced Photovoltaic Performance by Boosting Dielectric Constant and Carriers Kinetic Characteristics. *Macromol. Chem. Phys.* **2021**, *222* (12), 2100030.
(15) Tang, Y.; Xie, L.; Qiu, D.; Yang, C.; Liu, Y.; Shi, Y.; Huang, Z.; Zhang, J.; Hu, J.; Lu, K.; et al. Optimizing the Energy Levels and Crystallinity of 2,2′-Bithiophene-3,3′-Dicarboximide-Based Polymer Donors for High-Performance Non-Fullerene Organic Solar Cells. *J. Mater. Chem. C* **2021**, *9* (24), 7575-7582.
(16) Huang, J.; Peng, R.; Xie, L.; Song, W.; Hong, L.; Chen, S.; Wei, Q.; Ge, Z. A Novel Polymer Donor Based on Dithieno[2,3-D:2′,3′-D″]Benzo[1,2-B:4,5-B′]Dithiophene for Highly Efficient Polymer Solar Cells. *J. Mater. Chem. A* **2019**, *7* (6), 2646-2652.
(17) Zhang, M.; Zhu, L.; Guo, P.; Wang, X.; Tong, J.; Zhang, X.; Jia, Y.; Yang, R.; Xia, Y.; Wang, C. Effect of Flank Rotation on the Photovoltaic Properties of Dithieno[2,3-D:2′,3′-D′]Benzo[1,2-B:4,5-B′]Dithiophene-Based Narrow Band Gap Copolymers. *Polymers* **2019**, *11* (2), 239.
(18) Liu, T.; Huo, L.; Chandrabose, S.; Chen, K.; Han, G.; Qi, F.; Meng, X.; Xie, D.; Ma, W.; Yi, Y.; et al. Optimized Fibril Network Morphology by Precise Side-Chain Engineering to Achieve High-Performance Bulk-Heterojunction Organic Solar Cells. *Adv. Mater.* **2018**, *30* (26), 1707353.
(19) Gong, P.; Guo, P.; Wang, Y.; Yan, L.; Liang, Z.; Ding, M.; Tong, J.; Li, J.; Xia, Y. Ultrafast Kinetics Investigation of a Fluorinated-Benzothiadiazole Polymer with an Increased Excited State Transition Dipole Moment Applied in Organic Solar Cells. *ACS Appl. Energy Mater.* **2021**, *4* (9), 9627-9638.
(20) Lin, Y.; He, Q.; Zhao, F.; Huo, L.; Mai, J.; Lu, X.; Su, C.-J.; Li, T.; Wang, J.; Zhu, J.; et al. A Facile Planar Fused-Ring Electron Acceptor for as-Cast Polymer Solar Cells with 8.71% Efficiency. *J. Am. Chem. Soc.* **2016**, *138* (9), 2973-2976.
(21) Lin, Y.; Li, T.; Zhao, F.; Han, L.; Wang, Z.; Wu, Y.; He, Q.; Wang, J.; Huo, L.; Sun, Y.; et al. Structure Evolution of Oligomer Fused-Ring Electron Acceptors toward High Efficiency of as-Cast Polymer Solar Cells. *Adv. Energy Mater.* **2016**, *6* (18), 1600854.
(22) Lin, Y.; Zhao, F.; Wu, Y.; Chen, K.; Xia, Y.; Li, G.; Prasad, S. K. K.; Zhu, J.; Huo, L.; Bin, H.; et al. Mapping Polymer Donors toward High-Efficiency Fullerene Free Organic Solar Cells. *Adv. Mater.* **2017**, *29* (3), 1604155.
(23) Zhang, C.; Liu, T.; Zeng, W.; Xie, D.; Luo, Z.; Sun, Y.; Yang, C. Thienobenzene-Fused Perylene Bisimide as a Non-Fullerene Acceptor for Organic

Solar Cells with a High Open-Circuit Voltage and Power Conversion Efficiency. *Mater. Chem. Front.* **2017**, *1* (4), 749-756.
(24) Cai, Y.; Xue, X.; Han, G.; Bi, Z.; Fan, B.; Liu, T.; Xie, D.; Huo, L.; Ma, W.; Yi, Y.; et al. Novel Π-Conjugated Polymer Based on an Extended Thienoquinoid. *Chem. Mater.* **2018**, *30* (2), 319-323.
(25) Gao, P.; Tong, J.; Guo, P.; Li, J.; Wang, N.; Li, C.; Ma, X.; Zhang, P.; Wang, C.; Xia, Y. Medium Band Gap Conjugated Polymers from Thienoacene Derivatives and Pentacyclic Aromatic Lactam as Promising Alternatives of Poly(3-Hexylthiophene) in Photovoltaic Application. *J. Polym. Sci. Pol. Chem.* **2018**, *56* (1), 85-95.
(26) Liu, D.; Zhang, Y.; Zhan, L.; Lau, T.-k.; Yin, H.; Fong, P. W.-K.; So, S. K.; Zhang, S.; Lu, X.; Hou, J.; et al. Design of Wide-Bandgap Polymers with Deeper Ionization Potential Enables Efficient Ternary Non-Fullerene Polymer Solar Cells with 13% Efficiency. *J. Mater. Chem. A* **2019**, *7*, 14153-14162.
(27) Wang, X.; Han, J.; Jiang, H.; Liu, Z.; Li, Y.; Yang, C.; Yu, D.; Bao, X.; Yang, R. Regulation of Molecular Packing and Blend Morphology by Finely Tuning Molecular Conformation for High-Performance Nonfullerene Polymer Solar Cells. *ACS Appl. Mater. Interfaces* **2019**, *11* (47), 44501-44512.